J|A|C|S
ARTICLES

Published on Web 12/22/2008

Selective Synthesis of Single-Crystalline Rhombic Dodecahedral, Octahedral, and Cubic Gold Nanocrystals

Wenxin Niu,[†,‡] Shanliang Zheng,[§] Dawei Wang,[†,‡] Xiaoqing Liu,[†,‡] Haijuan Li,[†,‡] Shuang Han,[†,‡] Jiuan Chen,[†,‡] Zhiyong Tang,[*,§] and Guobao Xu[*,†]

State Key Laboratory of Electroanalytical Chemistry, Changchun Institute of Applied Chemistry, and Graduate University of the Chinese Academy of Sciences, Chinese Academy of Sciences, Changchun 130022, China, and National Center for Nanoscience and Technology, Beijing 100190, China

Received June 6, 2008; E-mail: zytang@nanoctr.cn.; guobaoxu@ciac.jl.cn

Abstract: This paper reports a versatile seed-mediated growth method for selectively synthesizing single-crystalline rhombic dodecahedral, octahedral, and cubic gold nanocrystals. In the seed-mediated growth method, cetylpyridinium chloride (CPC) and CPC-capped single-crystalline gold nanocrystals 41.3 nm in size are used as the surfactant and seeds, respectively. The CPC-capped gold seeds can avoid twinning during the growth process, which enables us to study the correlations between the growth conditions and the shapes of the gold nanocrystals. Surface-energy and kinetic considerations are taken into account to understand the formation mechanisms of the single-crystalline gold nanocrystals with varying shapes. CPC surfactants are found to alter the surface energies of gold facets in the order {100} > {110} > {111} under the growth conditions in this study, whereas the growth kinetics leads to the formation of thermodynamically less favored shapes that are not bounded by the most stable facets. The competition between $AuCl_4^-$ reduction and the CPC capping process on the {111} and {110} facets of gold nanocrystals plays an important role in the formation of the rhombic dodecahedral (RD) and octahedral gold nanocrystals. Octahedral nanocrystals are formed when the capping of CPC on {111} facets dominates, while RD nanocrystals are formed when the reduction of $AuCl_4^-$ on {111} facets dominates. Cubic gold nanocrystals are formed by the introduction of bromide ions in the presence of CPC. The cooperative work of cetylpyridinium and bromide ions can stabilize the gold {100} facet under the growth condition in this study, thereby leading to the formation of cubic gold nanocrystals.

1. Introduction

The properties of noble-metal nanocrystals are dictated by their sizes and shapes.[1−3] Therefore, size- and shape-controlled synthesis of noble-metal nanocrystals is essential for uncovering and understanding their intrinsic properties, which will consequently enable us to exploit them for catalytic, plasmonic, sensing, and spectroscopic applications.[1−6] Over the past decade, great progress has been made in crystallographic control over the nucleation and growth of gold nanocrystals. Most efforts thus far have been focused on the synthesis of octahedral and cubic gold nanocrystals bounded by {111} and {100} facets.[7−10] Synthesis of gold nanocrystals bounded by {110} facets has seldom been reported because the surface energy of the bare {110} facets is higher than those of bare {111} and {100} facets.[11] In principle, the shape of single-crystalline gold crystals bounded completely by equivalent {110} facets is supposed to be rhombic dodecahedral (RD),[12,13] i.e., such a crystal would be a convex polyhedron with 12 rhombic faces that has eight vertices where three faces meet at their obtuse angles and six vertices where four faces meet at their acute angles (Figure 1).[14] RD gold crystals have been observed in minerals,[12] and RD gold nano- and microcrystals have also been observed in chemical syntheses.[15,16] However, the rational synthesis of uniform RD gold nanocrystals in high yield has not been reported to date and is still a challenge that requires exquisite crystal-growth control.

Although several parameters have been revealed to greatly affect the growth mode of metal nanocrystals, the exact mechanisms for the shape-controlled synthesis of metal nanoc-

[†] Changchun Institute of Applied Chemistry.
[‡] Graduate University of the Chinese Academy of Sciences.
[§] National Center for Nanoscience and Technology.

(1) Murphy, C. J.; Sau, T. K.; Gole, A. M.; Orendorff, C. J.; Gao, J.; Gou, L.; Hunyadi, S. E.; Li, T. *J. Phys. Chem. B* **2005**, *109*, 13857.
(2) Wiley, B.; Sun, Y.; Xia, Y. *Acc. Chem. Res.* **2007**, *40*, 1067.
(3) Tao, A. R.; Habas, S.; Yang, P. *Small* **2008**, *4*, 310.
(4) Narayanan, R.; El-Sayed, M. A. *J. Am. Chem. Soc.* **2004**, *126*, 7194.
(5) Liz-Marzan, L. M. *Langmuir* **2006**, *22*, 32.
(6) Rosi, N. L.; Mirkin, C. A. *Chem. Rev.* **2005**, *105*, 1547.
(7) Kim, F.; Connor, S.; Song, H.; Kuykendall, T.; Yang, P. *Angew. Chem., Int. Ed.* **2004**, *43*, 3673.
(8) Sau, T. K.; Murphy, C. J. *J. Am. Chem. Soc.* **2004**, *126*, 8648.
(9) Seo, D.; Park, J. C.; Song, H. *J. Am. Chem. Soc.* **2006**, *128*, 14863.
(10) Li, C.; Shuford, K. L.; Park, Q.-H.; Cai, W.; Li, Y.; Lee, E. J.; Cho, O. C. *Angew. Chem., Int. Ed.* **2007**, *46*, 3264.
(11) Wang, Z. L. *J. Phys. Chem. B* **2000**, *104*, 1153.
(12) Taber, S. *Am. Mineral.* **1948**, *33*, 482.
(13) Francis, C. A. *Rocks Miner.* **2004**, *79*, 24.
(14) Weisstein, E. W. *CRC Concise Encyclopedia of Mathematics*, 2nd ed.; CRC Press: Boca Raton, FL, 2003; p 2546.
(15) Liu, X.; Wu, N.; Wunsch, B. H., Jr.; Stellacci, F. *Small* **2006**, *2*, 1046.
(16) Chen, Y.; Gu, X.; Nie, C.-G.; Jiang, Z.-Y.; Xie, Z.-X.; Lin, C.-J. *Chem. Commun.* **2005**, 4181.

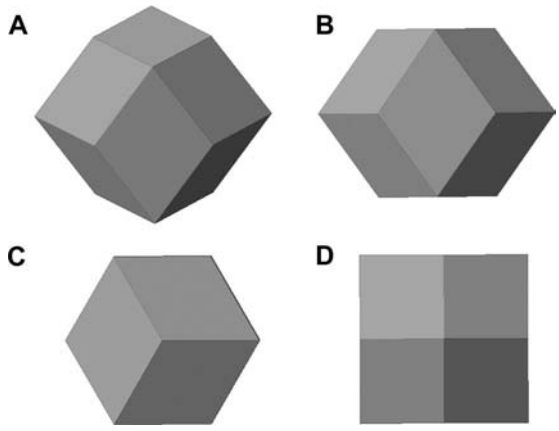

Figure 1. Geometrical models of rhombic dodecahedra: (A) overall view; (B) view perpendicular to one of the rhombic faces; (C) view centered on one of the vertices where three faces meet at their obtuse angles; (D) view centered on one of the vertices where four faces meet at their acute angles.

rystals are still not well-understood.[3] Most of the synthetic methods remain empirical, and understanding their growth mechanisms is still a challenging task. The seed-mediated growth method separates the nucleation and growth stages of nanocrystals, which provides better control over the size, size distribution, and shape evolution of the nanoparticles.[1,17] A typical seed-mediated growth process involves the preparation of small metal nanoparticles and their subsequent growth in reaction solutions containing metal salts, reducing agents, and surfactants. During the growth procedure, the crystal structures of the metal nanocrystals grown from small seeds are fluctuant.[18] The small seeds may grow into single-crystalline, twinned, or multitwinned structures,[19] leading to the formation of polydisperse nanostructures. The shape evolution of metal nanocrystals from seeds with different crystal structures is quite different,[20,21] which blurs our understanding of the mechanisms of the growth process. To preserve the single-crystalline nature of the seeds during the seed-mediated growth process, one has to judiciously select appropriate adsorbents[20,22] or manipulate the growth kinetics.[8] Therefore, development of a general strategy that can selectively produce single-crystalline metal nanocrystals without the need for elaborate selection of appropriate adsorbents or manipulation of the growth kinetics could enable us to study the detailed correlations between growth conditions and the shapes of the single-crystalline nanocrystals.

In this study, we developed a versatile seed-mediated growth method to selectively synthesize single-crystalline RD, octahedral, and cubic gold nanocrystals through manipulation of the growth kinetics and selection of appropriate adsorbates. Single-crystalline gold nanocrystals with diameters of 41.3 nm and capped by cetylpyridinium chloride (CPC) were prepared and explored as the seeds in the seed-mediated growth method. The single-crystalline nature and relatively large sizes of the CPC-capped seeds can fix the structure of the final nanocrystals as single-crystalline, enabling us to carefully study the parameters that affect the formation of the gold nanocrystals with varying shapes. Several important parameters that affect the shape evolutions of the gold nanocrystals are revealed, and the growth mechanisms are explained in terms of surface energy and growth kinetics.

2. Experimental Section

2.1. Materials. Chloroauric acid tetrahydrate ($HAuCl_4 \cdot 4H_2O$), sodium borohydride ($NaBH_4$), and cetyltrimethylammonium bromide (CTAB) were obtained from Sinopharm Chemical Reagent Co., Ltd. L-Ascorbic acid, silver nitrate ($AgNO_3$), and potassium bromide (KBr) were obtained from Beijing Chemical Reagent Company. CPC was obtained from Shanghai Sangon Company. All of the chemicals were of analytical grade and used without further purification. Doubly distilled water was used throughout the experiments.

2.2. Synthesis of Gold Nanorods. 2.2.1. Preparation of ~1.5 nm CTAB-Capped Gold Seeds. A 125 μL aliquot of 10 mM $HAuCl_4$ solution was added to 5 mL of 100 mM CTAB solution at 30 °C. After this combination was gently mixed, 0.3 mL of 10 mM ice-cold $NaBH_4$ solution was added all at once, followed by rapid inversion mixing for 2 min.[22,23] The CTAB-capped gold seed solution was stored at 30 °C for future use.

2.2.2. Synthesis of Gold Nanorods. In sequence, 2 mL of 10 mM $HAuCl_4$ solution, 240 μL of 10 mM $AgNO_3$ solution, 320 μL of freshly prepared 100 mM ascorbic acid solution, and 48 μL of the ~1.5 nm CTAB-capped gold seed solution were added to 40 mL of 100 mM CTAB solution at 30 °C. The solution was thoroughly mixed after each addition.[22,23] Finally, the gold nanorod solution was left undisturbed and aged for 2 h for further use.

2.3. Synthesis of the CPC-Capped Gold Seeds from Gold Nanorods. 2.3.1. Secondary Overgrowth of Gold Nanorods. A 30 mL aliquot of the as-synthesized gold nanorod solution was centrifuged (12 000 rpm, 10 min) and redispersed in water. Subsequently, the solution was centrifuged (12 000 rpm, 10 min) again and redispersed in 30 mL of 10 mM CTAB solution at 40 °C. Lastly, 1.5 mL of 10 mM $HAuCl_4$ solution and 0.3 mL of 100 mM ascorbic acid solution were added in sequence and mixed thoroughly. The mixture was allowed to react at 40 °C for 1 h.

2.3.2. Synthesis of the CPC-Capped Gold Seeds. The CPC-capped gold seeds were prepared by transformation of the overgrown gold nanorods to near-spherical nanoparticles.[24] Briefly, the overgrown gold nanorod solution was centrifuged (12 000 rpm, 10 min) and redispersed in 30 mL of 10 mM CTAB solution. Next, at 40 °C, 0.6 mL of 10 mM $HAuCl_4$ solution was added. After the solution was gently mixed, it was left undisturbed and aged for 12 h. The solution was then washed three times with 100 mM CPC solution by centrifugation (12 000 rpm, 10 min) and dissolution and finally dispersed in 30 mL of 100 mM CPC solution. We designated these nanoparticles as the CPC-capped seeds.

2.4. Seed-Mediated Growth of Three Types of Gold Nanocrystals. In a typical synthesis of the RD gold nanocrystals, 100 μL of 10 mM $HAuCl_4$ solution, 200 μL of freshly prepared 100 mM ascorbic acid solution, and 200 μL of the CPC-capped seed solution were added to 5 mL of 10 mM CPC solution at 30 °C in sequence. The solution was thoroughly mixed after each addition. The reaction was stopped after 2 h by centrifugation (12 000 rpm, 10 min). The gold nanocrystal solution was washed twice with water and concentrated for characterization by electron microscopy.

In a typical synthesis of the octahedral gold nanocrystals, 100 μL of 10 mM $HAuCl_4$ solution, 13 μL of freshly prepared 100 mM ascorbic acid solution, and 200 μL of the CPC-capped seed solution were added to 5 mL of 100 mM CPC solution at 30 °C in

(17) Murphy, C. J.; Gole, A. M.; Hunyadi, S. E.; Orendorff, C. J. *Inorg. Chem.* **2006**, *45*, 7544.
(18) Elechiguerra, J. L.; Reyes-Gasga, J.; Yacaman, J. M. *J. Mater. Chem.* **2006**, *16*, 3906.
(19) Wu, H.-Y.; Huang, W.-L.; Huang, M. H. *Cryst. Growth Des.* **2007**, *7*, 831.
(20) Liu, M.; Guyot-Sionnest, G. *J. Phys. Chem. B* **2005**, *109*, 22192.
(21) Lim, B.; Xiong, Y.; Xia, Y. *Angew. Chem., Int. Ed.* **2007**, *46*, 9279.
(22) Nikoobakht, B.; El-Sayed, M. A. *Chem. Mater.* **2003**, *15*, 1957.
(23) Sau, T. K.; Murphy, C. J. *Langmuir* **2004**, *20*, 6414.
(24) Rodriguez-Fernandez, J.; Perez-Juste, J.; Mulvaney, P.; Liz-Marzan, L. M. *J. Phys. Chem. B* **2005**, *109*, 14257.

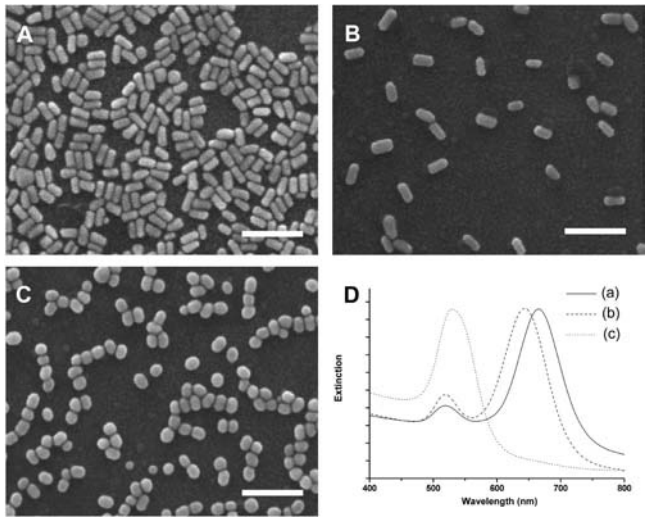

Figure 2. SEM images of (A) the gold nanorods, (B) the overgrown gold nanorods, and (C) the CPC-capped gold seeds (scale bars: 200 nm). (D) UV−vis extinction spectra of (a) the gold nanorods, (b) the overgrown gold nanorods, and (c) the CPC-capped gold seeds (each spectrum is normalized against the intensity of its strongest peak).

sequence. The solution was thoroughly mixed after each addition. The reaction was stopped after 2 h by centrifugation (12 000 rpm, 10 min).

In a typical synthesis of the cubic gold nanocrystals, 500 μL of 100 mM KBr solution, 100 μL of 10 mM $HAuCl_4$ solution, 13 μL of freshly prepared 100 mM ascorbic acid solution, and 200 μL of the CPC-capped seed solution were added to 5 mL of 100 mM CPC solution at 30 °C in sequence. The solution was thoroughly mixed after each addition. The reaction was stopped after 2 h by centrifugation (12 000 rpm, 10 min).

2.5. Instrumentation. Scanning electron microscopy (SEM) images were taken using an FEI XL30 ESEM FEG scanning electron microscope operating at 25 kV. Transmission electron microscopy (TEM) and selected-area electron diffraction (SAED) studies were performed on a FEI Tecnai G^2 20 S-TWIN transmission electron microscope operated at 200 kV. A drop of the concentrated nanocrystal solution was deposited on ITO glass or a TEM grid for SEM or TEM measurements, respectively. During natural evaporation of water, part of the nanocrystals migrated to the edge of the drop and formed a solid ring. SEM observations revealed that ordered assemblies mainly existed at the coffee-ring region, while random assemblies mainly existed at the center. UV−vis extinction spectra were taken at room temperature on a CARY 500 Scan UV−vis−near-IR spectrophotometer using a quartz cuvette with an optical path of 1 cm. X-ray diffraction (XRD) measurements were obtained with a Rigaku D/MAX-2500 instrument (Cu $K\alpha_1$ radiation) operated at 50 kV and 250 mA over a range of 30−90° by step scanning with a step size of 0.02°.

3. Results and Discussion

3.1. Preparation and Characterization of the CPC-Capped Gold Seeds. Gold nanorods were overgrown and then oxidized by Au(III)−CTAB complexes to prepare the CPC-capped gold seeds. The oxidation occurred preferentially at the ends of the overgrown gold nanorods and eventually led to the formation of near-spherical nanoparticles.[24] These near-spherical nanoparticles were finally dispersed in 100 mM CPC solution and designated as the CPC-capped gold seeds. As shown in Figure 2, the average width, length, and aspect ratio of the gold nanorods are 27.2 nm, 58.8 nm, and 2.2, respectively, and the average width, length, and aspect ratio of the overgrown gold nanorods are 32.4 nm, 63.7 nm, and 2.0, respectively; the CPC-capped gold seeds have an average diameter of 41.3 nm and a size distribution of 5.4%. The detailed morphology and structures of the CPC-capped seeds were studied through TEM. Figure 3A shows that the shapes of the CPC-capped gold seeds are slightly ellipsoidal rather than perfectly spherical. Therefore, the average diameter of the seeds is bigger than the average width of the overgrown nanorods from which they originate. The SAED pattern and high-resolution TEM (HRTEM) image of a single CPC-capped seed demonstrate that the CPC-capped seeds are single-crystalline (Figure 3B,C). The process of preparing the CPC-capped seeds was also studied by UV−vis spectroscopy. The UV−vis extinction spectra of the gold nanorods, overgrown gold nanorods, and CPC-capped seeds are shown in Figure 2D. The two peaks in the UV−vis extinction spectra of the gold nanorods and overgrown gold nanorods can be attributed to the transverse and longitudinal plasmon modes of gold nanorods.[22] The blue shift in the longitudinal plasmon mode of the overgrown nanorods confirms a decrease in their aspect ratios.[25] The UV−vis extinction spectrum of the CPC-capped seeds has only one peak [curve (c) in Figure 2D], which confirms their near-spherical morphology.

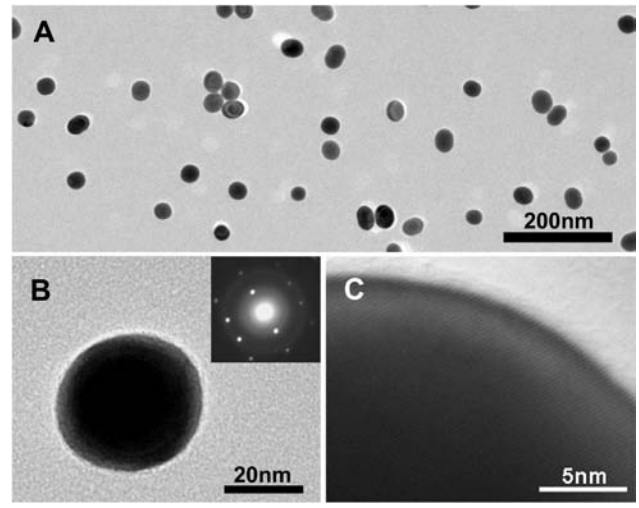

Figure 3. (A) TEM image of the CPC-capped gold seeds. (B) TEM image and corresponding SAED pattern of a single CPC-capped seed. (C) HRTEM image of the CPC-capped seed in (B).

3.2. Synthesis of Single-Crystalline RD, Octahedral, and Cubic Gold Nanocrystals. 3.2.1. Synthesis and Characterization of RD Gold Nanocrystals. Synthesis of RD gold nanocrystals was performed at 30 °C. Typically, 100 μL of 10 mM $HAuCl_4$ solution, 200 μL of 100 mM ascorbic acid solution, and 200 μL of the CPC-capped seed solution were added to 5 mL of 10 mM CPC solution in sequence. The reaction was stopped after 2 h by centrifugation. Figure 4A,B shows SEM images of orderly assembled and randomly distributed RD gold nanocrystals, respectively. In the ordered assembly of RD gold nanocrystals, the RD gold nanocrystals are in the orientation shown in Figure 1C. From the randomly distributed RD gold nanocrystals, the geometrical shapes of these gold nanocrystals can be viewed from different directions and identified as RD, i.e., bounded by 12 equivalent rhombic faces (Figure S1 in the Supporting Information).[14] Figure 4C shows the TEM image of the RD gold nanocrystals. Most of the RD nanocrystals tend to lie flat and exhibit elongated hexagonal shapes. For a flat-

(25) Tsung, C.-K.; Kou, X.; Shi, Q.; Zhang, J.; Yeung, M. H.; Wang, J.; Stucky, G. D. *J. Am. Chem. Soc.* **2006**, *128*, 5352.

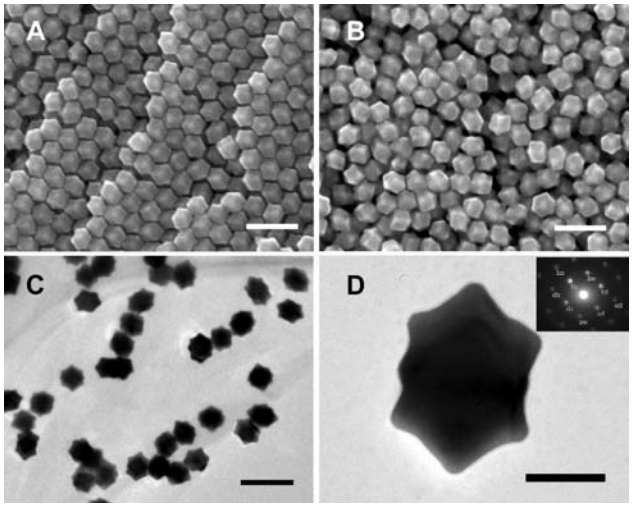

Figure 4. SEM images of (A) orderly assembled and (B) randomly distributed RD gold nanocrystals (scale bars: 200 nm). (C) TEM image of the RD gold nanocrystals (scale bar: 200 nm). (D) TEM image and corresponding SAED pattern of a single flat-lying RD gold nanocrystal recorded along the [011] zone axis (scale bar: 50 nm).

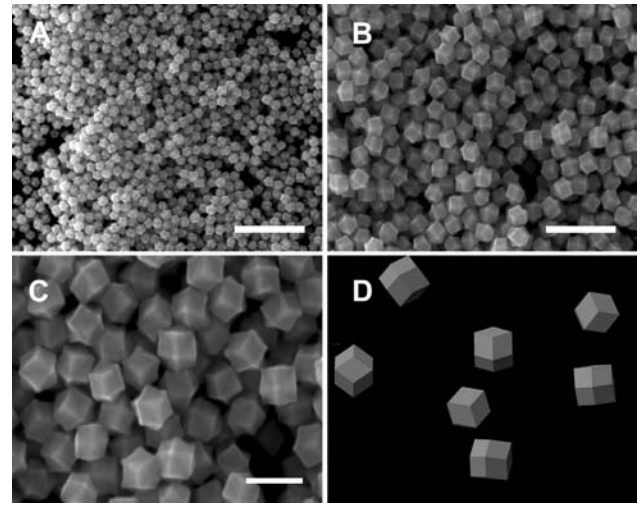

Figure 5. SEM images of larger RD gold nanocrystals at different magnifications [scale bars: (A) 1 μm, (B) 500 nm, (C) 200 nm]. (D) RD geometrical models with typical orientations corresponding to RD gold nanocrystals at the same positions in (C).

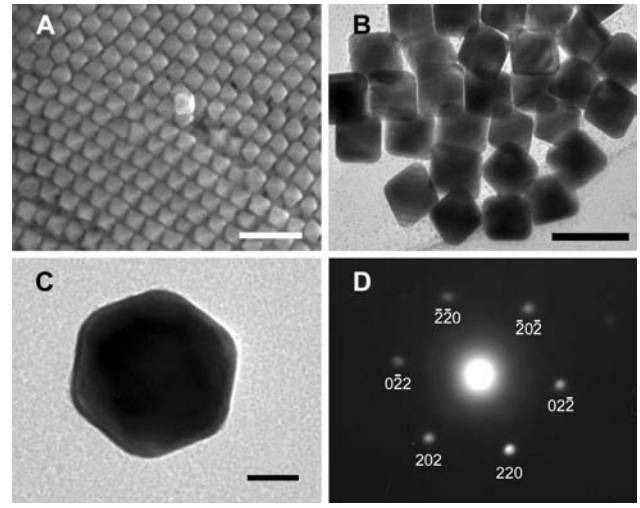

Figure 6. (A) SEM image of octahedral gold nanocrystals (scale bar: 200 nm). (B) TEM image of octahedral gold nanocrystals (scale bar: 100 nm). (C) TEM image and (D) corresponding SAED pattern of a single flat-lying octahedral gold nanocrystal recorded along the [$\bar{1}$11] zone axis (scale bar: 20 nm).

lying RD gold nanocrystal, the top and bottom {110} faces of the RD gold nanocrystal are parallel to the substrate. Directing the electron beam perpendicular to the upper face of the flat-lying RD nanocrystal produces the typical SAED pattern of a gold crystal along the [011] zone axis,[12,13,26] as shown in the inset of Figure 4D. The HRTEM and corresponding SAED images of gold nanocrystals viewed from different directions further confirm their RD shapes (Figure S2 in the Supporting Information). It should be pointed out that the XRD pattern of the RD gold nanocrystals (Figure S3 in the Supporting Information) does not have an abnormally intense (220) peak because SEM observations (Figure 4A,B) reveal that not all of the RD nanocrystals lie flat on the substrate.

The TEM image in Figure 4D also reveals that the corners of the RD gold nanocrystal are slightly stretched-out, which indicates that the faces of the RD nanocrystals are not perfectly flat. In order to clearly distinguish the surface morphologies of the RD nanocrystals, larger RD nanocrystals were also synthesized by reducing the added volume of the seed solution to 25 μL. As shown in Figure 5, the faces of the RD nanocrystals are concave with relatively flat center parts parallel to the ideal {110} facets. Therfore, although the gold nanocrystals in Figures 4 and 5 take an RD overall shape, their faces are not perfect {110} facets, and the center part of each facet is supposed to be a {110} facet.

3.2.2. Synthesis and Characterization of Octahedral Gold Nanocrystals. Octahedral gold nanocrystals were synthesized under conditions similar to those for the synthesis of the RD gold nanocrystals in Figure 4, except that the concentration of CPC was increased from 10 to 100 mM and the volume of 100 mM ascorbic acid solution was decreased from 200 to 13 μL. SEM and TEM images of the octahedral gold nanocrystals are presented in Figure 6A,B, respectively. The SAED study indicates that the octahedral gold nanocrystal is a piece of single crystal bounded by {111} facets (Figure 6C,D).[9,10]

3.2.3. Synthesis and Characterization of Cubic Gold Nanocrystals. Cubic gold nanocrystals were produced when 0.5 mL of 100 mM KBr solution was introduced while the other conditions were kept the same as those in the synthesis of the octahedral gold nanocrystals. Figure 7A,B shows the SEM and TEM images of the cubic gold nanocrystals, respectively, and Figure 7C,D shows the TEM image and corresponding SAED pattern of a single cubic gold nanocrystal. The square spot array of the SAED pattern indicates that the cubic gold nanocrystal is a single crystal bounded by {100} facets.[7,9] Cubic gold nanocrystals are also produced when only 0.05 mL of 100 mM KBr solution is introduced, as shown in Figure S4 in the Supporting Information.

3.2.4. Average Edge Lengths, Size Distributions, Yields, and Corresponding Optical Properties of the Gold Nanocrystals. Table 1 summarizes the average sizes, size distributions, and yields of the gold nanocrystals presented in Figures 4, 6, and 7. All three types of gold nanocrystals are prepared in high yields with good monodispersity. Compared with the CPC-capped seeds, the final nanocrystals have improved monodis-

(26) Wang, Z. L. *Reflection Electron Microscopy and Spectroscopy for Surface Analysis*; Cambridge University Press: Cambridge, U.K., 1996; Appendix D.

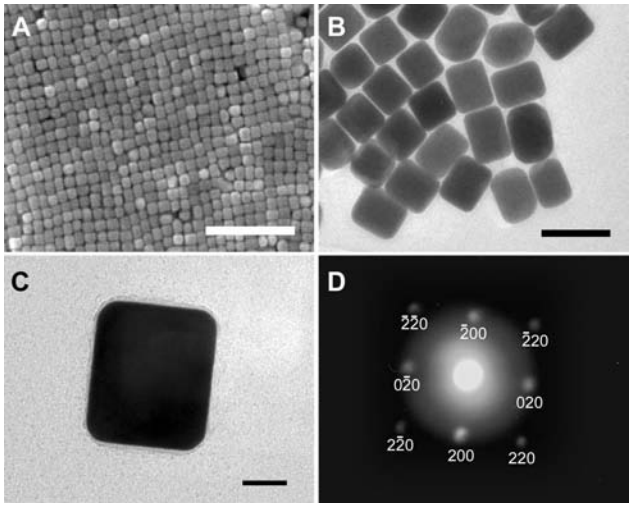

Figure 7. (A) SEM image of cubic gold nanocrystals (scale bar: 500 nm). (B) TEM image of cubic gold nanocrystals (scale bar: 100 nm). (C) TEM image and (D) corresponding SAED pattern of a single flat-lying cubic gold nanocrystal recorded along the [001] zone axis (scale bar: 20 nm).

Table 1. Average Edge Lengths (L_{av}), Size Distribution Standard Deviations (σ), and Yields of the RD, Octahedral, and Cubic Gold Nanocrystals

shape	L_{av} (nm)	σ (%)	yield (%)	figure no.
RD	53.4	5.3	~100	4
octahedral	59.8	4.1	97.2	6
cubic	55.7	4.4	96.1	7

persity. In seed-mediated growth procedures, the improvement in the monodispersity is attributed to the "self-focusing" tendency that small particles grow faster than larger ones, causing the final sizes of the nanocrystals to become uniform.[27,28] Such observations are consistent with previous reports that the monodispersity of the grown nanoparticles is better than that of the seeds.[29−31] It is well-known that noble metal nanoparticles exhibit size- and shape-dependent optical properties arising from surface plasmon resonances.[32] As shown in Figure 8, the UV−vis extinction spectra of the RD, octahedral, and cubic gold nanocrystals show peaks at 582, 568, and 551 nm, respectively. The differences in the UV−vis extinction spectra may result from the differences in the sizes, shapes, and outstretched or truncated corners of the gold nanocrystals.

3.3. Growth Mechanisms of the Gold Nanocrystals. In a seed-mediated growth procedure, several parameters are simultaneously responsible for the final shapes of the gold nanocrystals.[17] Hence several control experiments are conducted to elucidate the growth mechanisms of the gold nanocrystals. In the nucleation stage, the size and crystal structure of seeds are proved to be important for the formation of single-crystalline structures of the gold nanocrystals. In the growth stage, surfactants, growth kinetics, and adsorbates are found to determine the final shapes of the resultant single-crystalline gold nanocrystals.

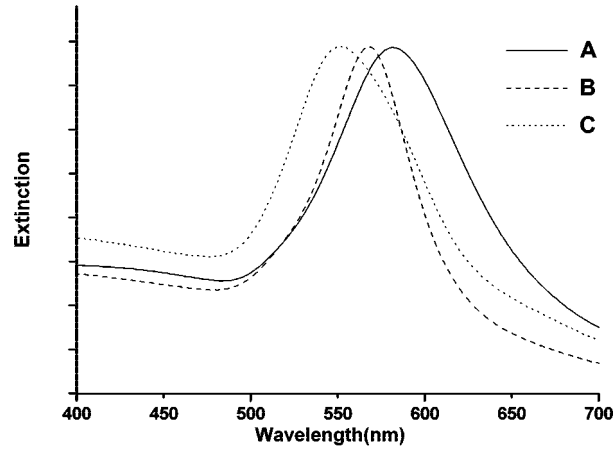

Figure 8. UV−vis extinction spectra of (A) the RD gold nanocrystals in Figure 4, (B) the octahedral gold nanocrystals in Figure 6, and (C) the cubic gold nanocrystals in Figure 7 (each spectrum is normalized against the intensity of its strongest peak).

3.3.1. The Importance of the Size and Crystal Structure of the Seeds. To investigate how the size and crystal structure of the seeds affect the growth of gold nanocrystals, another two types of seeds commonly used in the seed-mediated growth method were adopted here (under the same growth conditions) in addition to the CPC-capped gold seeds. These two types of seeds were ~3 nm citrate-capped twinned gold seeds and ~1.5 nm CTAB-capped single-crystalline gold seeds.[20] Among the three types of seeds, the ~1.5 nm CTAB-capped single-crystalline seed solution contains bromide ions, and bromide ions from this seed solution may affect the growth of gold nanocrystals.[33] Therefore, we intentionally adopted the growth conditions with the addition of KBr to counteract the influence of the presence or absence of bromide ions in different seed solutions.

SEM images of the gold nanocrystals synthesized with the different types of seeds are shown in Figure 9, and their corresponding shape distributions are summarized in Table S1 in the Supporting Information. When the CPC-capped single-crystalline gold seeds were used, cubic gold nanocrystals were produced in high yield (95.2%). In contrast, only 4.0% of the products were cubic nanocrystals when the ~3 nm twinned nanoparticles were used, and 26.1% of the products were cubic nanocrystals when ~1.5 nm single-crystalline nanoparticles were used. These results provide evidence that both the single-crystalline nature and the relatively large sizes of the CPC-capped seeds play important roles in the growth of single-crystalline gold nanocrystals with high yields. It is believed that the crystal structure of the seeds fluctuates at very small sizes, whereas their structure will be fixed as single-crystalline or multitwinned as the size of the crystals increases.[18,34] Because of their relatively large sizes, the CPC-capped single-crystalline seeds can avoid twinning during the growth process, enabling us to study the parameters that affect the growth of the gold nanocrystals. It should also be noted that the present procedure for preparing the CPC-capped seeds is somewhat tedious. Ongoing efforts in our group are being directed toward finding simpler methods for synthesis of high-quality single-crystalline gold seeds with relatively large sizes.

(27) Reiss, H. *J. Chem. Phys.* **1951**, *19*, 482.
(28) Peng, X. G.; Wickham, J.; Alivisatos, A. P. *J. Am. Chem. Soc.* **1998**, *120*, 5343.
(29) Brown, K. R.; Walter, D. G.; Natan, M. J. *Chem. Mater.* **2000**, *12*, 306.
(30) Henglein, A. *Langmuir* **1999**, *15*, 6738.
(31) Jana, N. R.; Gearheart, L.; Murphy, C. J. *Langmuir* **2001**, *17*, 6782.
(32) Xia, Y.; Halas, N. J. *MRS Bull.* **2005**, *30*, 338.
(33) Ha, T. H.; Koo, H. J.; Chung, B. H. *J. Phys. Chem. C* **2007**, *111*, 1123.
(34) Im, S. H.; Lee, Y. T.; Wiley, B.; Xia, Y. *Angew. Chem., Int. Ed.* **2005**, *44*, 2154.

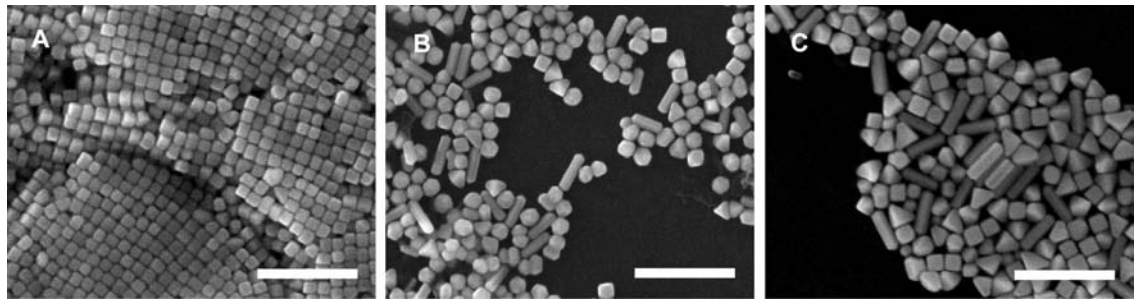

Figure 9. SEM images of gold nanocrystals synthesized with different types of seeds: (A) 41.3 nm CPC-capped single-crystalline gold seeds; (B) ~3 nm citrate-capped twinned gold seeds; (C) ~1.5 nm CTAB-capped single-crystalline gold seeds (all scale bars: 500 nm). The gold nanocrystals were synthesized by adding 50 μL of 100 mM KBr solution, 100 μL of 10 mM $HAuCl_4$ solution, 15 μL of 100 mM ascorbic acid solution, and the corresponding amount of seed solution (200 μL for the CPC-capped seed solution, 1 μL for the ~3 nm citrate-capped twinned seed solution, and 0.02 μL for the ~1.5 nm CTAB-capped single-crystalline seed solution) to 5 mL of 100 mM CPC solution at 30 °C.

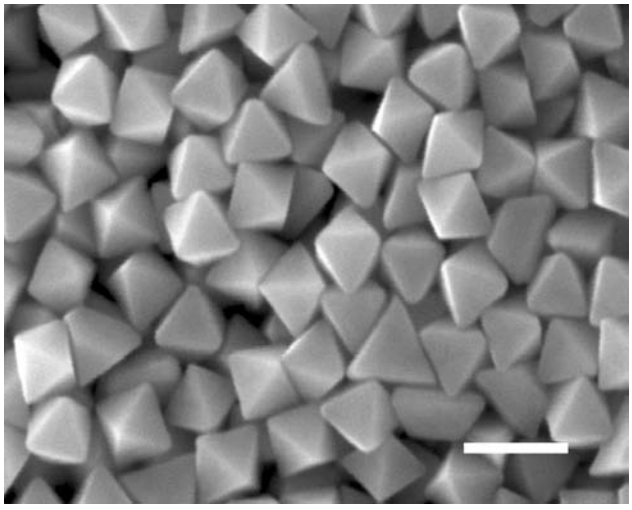

Figure 10. SEM image of larger octahedral gold nanocrystals synthesized with 25 μL of the CPC-capped seed solution added (scale bar: 200 nm).

3.3.2. Surface Energies of Different Gold Crystallographic Facets in the Presence of CPC. Surface energies associated with different gold crystallographic facets usually increase in the order $\gamma_{\{111\}} < \gamma_{\{100\}} < \gamma_{\{110\}}$.[11,35] In a solution-phase synthesis, adsorbates (including surfactants, polymers, small molecules, and atomic adsorbates) can interact selectively with different metal crystal facets and alter their surface energies.[3] It has been reported that gold nanorods have {110} side facets.[20,36] These {110} facets disappear during overgrowth in the presence of CTAB or poly(vinyl pyrrolidone).[37,38] In contrast, CPC can selectively stabilize the {110} facets of gold, and thus, RD gold nanocrystals can exist as final products. The preparation of octahedral gold nanocrystals indicates that CPC can also stabilize the {111} facets of gold. Through a comparison between the surface structures of the larger RD and octahedral gold nanocrystals shown in Figures 5 and 10, respectively, we found that the faces of the octahedral gold nanocrystals are flat and smooth but that the faces of the RD gold nanocrystals are not well-defined {110} facets, which suggests that CPC stabilizes {110} facets relatively poorly. Moreover, octahedral gold nanocrystals bounded by {111} facets are obtained at relatively high CPC concentrations, suggesting that the enhanced capping of CPC promotes the formation of {111} facets of gold. These observations suggest that the gold {111} facets should be more stable than gold {110} facets in the presence of CPC under the growth conditions in this study. Since gold nanocrystals bounded by {100} facets are not observed in the presence of CPC, we suppose that gold {100} facets tend to disappear during the growth procedure, and it should be the most unstable low-index facet of gold in the presence of CPC. Therefore, it is reasonable to assume that CPC alters the surface energies of gold facets, ordering them as $\gamma_{\{111\}} < \gamma_{\{110\}} < \gamma_{\{100\}}$ under the growth conditions in this study. The selective interactions of CPC with different gold facets are responsible for the alteration.

3.3.3. Growth Kinetics of the RD and Octahedral Gold Nanocrystals. The above surface-energy considerations suggest that the RD gold nanocrystal is not the thermodynamically most favored shape. The formation of thermodynamically less favored shapes of nanocrystals are generally governed by growth kinetics.[39−41] In the case of the selective synthesis of RD and octahedral gold nanocrystals, growth kinetics and the capping effect of CPC must be taken into account simultaneously in order to understand their growth mechanisms.

Several control experiments were conducted to investigate the formation mechanisms of RD and octahedral gold nanocrystals. RD gold nanocrystals could still be prepared when the concentration of CPC was increased to 100 mM and the volume of 100 mM ascorbic acid solution was between 200 and 25 μL, while other conditions were the same as those in the synthesis of the RD gold nanocrystals in Figure 4. The corresponding SEM images of the RD nanocrystals are shown in Figure 11A,B. When the volume of ascorbic acid solution was further reduced to 13 μL, octahedral gold nanocrystals were produced, as shown in Figure 6. These results indicate that the competition between $AuCl_4^-$ reduction and the CPC capping process on the {111} and {110} surfaces plays an important role. Octahedral gold nanocrystals bounded by {111} facets were obtained at relatively high CPC concentrations, suggesting that the capping of CPC promotes the formation of {111} facets of gold. At relatively high ascorbic acid concentrations, RD nanocrystals were

(35) Xiong, Y.; Wiley, B.; Xia, Y. *Angew. Chem., Int. Ed.* **2007**, *46*, 7157.
(36) Wang, Z. L.; Mohamed, M. B.; Link, S.; El-Sayed, M. A. *Surf. Sci.* **1999**, *440*, L809.
(37) Xiang, Y.; Wu, X.; Liu, D.; Feng, L.; Zhang, K.; Chu, W.; Zhou, W.; Xie, S. *J. Phys. Chem. C* **2008**, *112*, 3203.
(38) Carbo-Argibay, E.; Rodriguez-Gonzalez, B.; Pacifico, J.; Pastoriza-Santos, I.; Perez-Juste, J.; Liz-Marzan, L. M. *Angew. Chem., Int. Ed.* **2007**, *46*, 8983.
(39) Petroski, J. M.; Wang, Z. L.; Green, T. C.; El-Sayed, M. A. *J. Phys. Chem. B* **1998**, *102*, 3316.
(40) Xiong, Y.; Cai, H.; Wiley, B. J.; Wang, J.; Kim, M. J.; Xia, Y. *J. Am. Chem. Soc.* **2007**, *129*, 3665.
(41) Tao, A.; Sinsermsuksakul, P.; Yang, P. *Angew. Chem., Int. Ed.* **2006**, *45*, 4597.

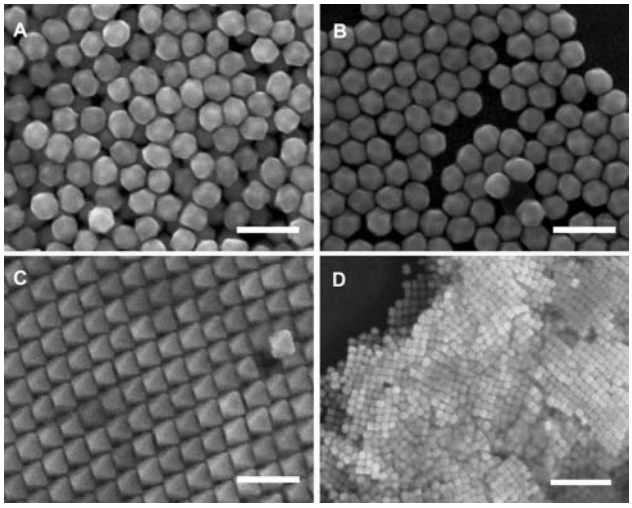

Figure 11. SEM images of gold nanocrystals: (A) RD nanocrystals synthesized with 200 μL of 100 mM ascorbic acid in 100 mM CPC solution at 30 °C (scale bar: 200 nm); (B) RD nanocrystals synthesized with 25 μL of 100 mM ascorbic acid in 100 mM CPC solution at 30 °C (scale bar: 200 nm); (C) octahedral nanocrystals synthesized with 25 μL of 100 mM ascorbic acid in 100 mM CPC solution at 20 °C (scale bar: 200 nm); (D) cubic nanocrystals synthesized in 10 mM CTAB solutions with 13 μL of 100 mM ascorbic acid at 30 °C by using the CTAB-capped 41.3 nm single-crystalline seeds (scale bar: 500 nm).

obtained, which suggests that the reduction of $AuCl_4^-$ by ascorbic acid tends to occur on the {111} facets of gold, leading to the disappearance of {111} facets and the formation of {110} facets. Therefore, octahedral gold nanocrystals are formed when the capping of CPC on {111} facets dominates, while RD gold nanocrystals are formed when the reduction of $AuCl_4^-$ on {111} facets dominates.

The reaction temperature can also affect the growth kinetics of the gold nanocrystals. As shown in Figure 11C, octahedral gold nanocrystals were produced when the reaction temperature was decreased from 30 to 20 °C while the other conditions were the same as those in the synthesis of the RD gold nanocrystals shown in Figure 11B. A decrease in reaction temperature can slow down the reduction of $AuCl_4^-$ ions by ascorbic acid. The reaction rate in our system was estimated to increase ~3.3 times as the reaction temperature was increased from 20 to 30 °C, according to the results of Zijlstra et al.[42] and the Arrhenius equation. Low temperature can also favor the adsorption of CPC.[43] Both the retarded reduction of $AuCl_4^-$ on the {111} facets of gold and the increased capping of CPC on {111} facets of gold promote the production of octahedral gold nanocrystals bounded by {111} facets, which is in accordance to the growth mechanisms we proposed above.

3.3.4. Effect of Bromide Ions. The adsorption of cationic surfactants based on quaternary ammonium cations onto a gold surface is mediated by the precedent-specific adsorption of halide counterions.[33] In the case of CPC, chloride counterions adsorb onto the gold surface and create a negatively charged layer, after which cetylpyridinium cations adsorb onto the surface through electrostatic forces.[44] When KBr is introduced into the growth solution, the bromide ions replace the chloride ions and mediate the adsorption of cetylpyridinium cations, since bromide ion has a higher affinity for gold than chloride ion does.[45] Several reports suggest that cationic surfactants with bromide counterions can stabilize the {100} facets of noble metals by reducing their surface energies,[46−48] and the cooperative work of cetylpyridinium and bromide ions plays a similar role herein. By using the CPC-capped single-crystalline seeds, twinning was avoided during the growth process, and therefore, cubic gold nanocrystals with single-crystalline structures bounded by {100} facets were formed.

CTAB is also a cationic surfactant with bromide counterions and is widely used in seed-mediated growth methods.[1] It has been reported that CTAB can stabilize the {100} facets of gold.[46] To investigate whether CTAB plays a similar role in the growth method presented here, CPC was replaced with CTAB as the surfactant. CTAB-capped single-crystalline gold seeds 41.3 nm in size were prepared by a process similar to that for the CPC-capped seeds, except that the seeds were finally dispersed in 100 mM CTAB solution. Figure 11D shows that cubic gold nanocrystals were also obtained as final products when the CTAB-capped 41.3 nm seeds were used. Therefore, CTAB plays a role similar to that of the cooperative work of cetylpyridinium and bromide ions under the growth conditions in this study.

4. Conclusion

In conclusion, we report a versatile method to selectively synthesize single-crystalline rhombic dodecahedral, octahedral, and cubic gold nanocrystals. This is also the first report regarding the rational synthesis of RD gold nanocrystals in high yield. Parameters that are responsible for the final shapes of the gold nanocrystals have been studied in detail. The adoption of the CPC-capped gold seeds enabled us to temporarily ignore the elusive nucleation process in typical growth processes of metal nanocrystals, and thus, it was possible to study the correlations between the growth conditions and the shapes of the gold nanocrystals in the growth process. During the growth process, important parameters, including surfactants, growth kinetics, and adsorbates, were found to affect the shape formation of the gold nanocrystals, and the growth mechanisms are explained in terms of surface energy and growth kinetics. These results may provide a foundation for gaining mechanistic insights into the growth of shape- and structure-controlled noble-metal nanocrystals.

Acknowledgment. We gratefully acknowledge support from the National Natural Science Foundation of China (20875086 for G.X.; 20773033 for Z.T.), the Department of Sciences & Technology of Jilin Province (20070108), the Ministry of Science and Technology of the People's Republic of China (2006BAE03B08), the National Research Fund for Fundamental Key Projects (2009CB930401), and the Hundred Talents Program of the Chinese Academy of Sciences (G.X. and Z.T.). We thank M. Y. Li and Y. D. Fan for technical assistance and helpful discussions.

Supporting Information Available: Figures S1−S4 and Table S1. This material is available free of charge via the Internet at http://pubs.acs.org.

JA804115R

(42) Zijlstra, P.; Bullen, C.; Chon, J. W. M.; Gu, M. *J. Phys. Chem. B* **2006**, *110*, 19315.
(43) Wittrock, C.; Kohler, H.-H.; Seidel, J. *Langmuir* **1996**, *12*, 5550.
(44) Jang, N. H. *Bull. Korean Chem. Soc.* **2004**, *25*, 1392.
(45) Magnussen, O. M. *Chem. Rev.* **2002**, *102*, 679.
(46) Johnson, C. J.; Dujardin, E.; Davis, S. A.; Murphy, C. J.; Mann, S. *J. Mater. Chem.* **2002**, *12*, 1765.
(47) Yu, D. B.; Yam, V. W. W. *J. Am. Chem. Soc.* **2004**, *126*, 13200.
(48) Zhang, Y.; Grass, M. E.; Kuhn, J. N.; Tao, F.; Habas, S. E.; Huang, W.; Yang, P.; Somorjai, G. A. *J. Am. Chem. Soc.* **2008**, *130*, 5868.